

# Influence of an inhomogeneous internal magnetic field on the flow dynamics of a ferrofluid between differentially rotating cylinders

S. Altmeyer\* and Younghae Do†

*Department of Mathematics, Kyungpook National University, Daegu 702-701, Korea*

J. M. Lopez‡

*School of Mathematical and Statistical Sciences, Arizona State University, Tempe, Arizona 85202, USA and Department of Mathematics, Kyungpook National University, Daegu 702-701, Korea*

(Received 2 April 2012; published 19 June 2012)

The influence of a magnetic field on the dynamics of the flow of a ferrofluid in the gap between two concentric, independently rotating cylinders is investigated numerically. The Navier-Stokes equations are solved using a hybrid finite difference and Galerkin method. We show that the frequently used assumption that the internal magnetic field within a ferrofluid is equal to the external applied field is only a leading-order approximation. By accounting for the ferrofluid's magnetic susceptibility, we show that a uniform externally imposed magnetic field is modified by the presence of the ferrofluid within the annulus. The modification to the magnetic field has an  $r^{-2}$  radial dependence and a magnitude that scales with the susceptibility. For ferrofluids typically used in laboratory experiments of the type simulated in this paper, the modification to the imposed magnetic field can be substantial. This has significant consequences on the structure and stability of the basic states, as well as on the bifurcating solutions.

DOI: [10.1103/PhysRevE.85.066314](https://doi.org/10.1103/PhysRevE.85.066314)

PACS number(s): 47.65.Cb, 47.20.Ky

## I. INTRODUCTION

There has been much interest recently in the use of ferrofluids [1] in a wide variety of applications, ranging from their use in computer hard drives and as liquid seals in rotating systems to their use in laboratory experiments to study geophysical flows [2,3]. Deeper fundamental study of their magnetohydrodynamics is inevitable, as there are many modeling assumptions that have been implemented to make theoretical descriptions tractable.

Ferrofluids are manufactured fluids consisting of dispersions of magnetized nanoparticles in a variety of liquid carriers. They are stabilized against agglomeration by the addition of a surfactant monolayer onto the particles. In the absence of an applied magnetic field, the magnetic nanoparticles are randomly orientated, the fluid has zero net magnetization, and the presence of the nanoparticles provides a typically small alteration to the fluid's viscosity and density. When a sufficiently strong magnetic field is applied, the ferrofluid flows toward regions of the magnetic field, properties of the fluid such as the viscosity are altered, and the hydrodynamics of the system can be significantly changed.

Most models describing the hydrodynamics of ferrofluids in containers assume that the internal magnetic field within the fluid is equal to the external applied field [4–6]. Depending on the magnetic susceptibility of the ferrofluid held in the container, the magnetic field is modified from the external field, providing a much changed body force in the governing equations.

As a prototypical system to investigate the influences of a magnetic field on a rotating ferrofluid system, we consider

Taylor-Couette flow driven by the differential rotation of two concentric cylinders. There are many theoretical and experimental analyses of the influence of symmetric magnetic fields in various configurations on the flow of a ferrofluid in the Taylor-Couette system [4–12]. Most of these have focused on the relaxation phenomena of magnetic particles. Debye [13] presents one of the first theories on magnetic relaxation, describing a balance between the magnetic torque on the particles and the mechanical braking torque due to the fluid viscosity. Shliomis and coworkers have made various extensions to this theory. Their first extension [14,15] includes an expression for the angular velocity of the ferrofluid particles, which is not the same as that of the ferrofluid itself due to the magnetic torques acting on the particles. To account for the differences in the angular velocities, they define a mean particle angular velocity. The second extension [16,17] also uses a mean particle angular velocity but considers the relaxation phenomenon from the standpoint of an effective field, defined as the component of the magnetic field along the direction of the magnetization. Müller and Liu [18] describe a more general structure of the hydrodynamic equations, with the Debye and Shliomis theories being special cases. The effective field theory was also used by Felderhof [19], who further introduced vortex viscosity as a new additional parameter to account for the increase in viscosity of a ferrofluid due to an applied magnetic field. Odenbach and Müller [20] investigated experimentally the nonequilibrium magnetization of a ferrofluid in the Taylor-Couette system subjected to a homogeneous transverse magnetic field. Their results reveal that the symmetric velocity gradient significantly affects the magnetization vector in the ferrofluid.

Numerical simulations as well as experiments show that any axisymmetric applied magnetic field, whether radial, axial, or any combination, stabilizes the basic state [4,6,12,21,22]. This stabilization effect depends, among others, on the

\*sebastianaltmeyer@t-online.de

†yhdo@knu.ac.kr

‡jmlopez@asu.edu

particle-particle interactions of the fluid [22]. A strong interaction leads to large changes in flow behavior, which are driven by the formation of internal flow structures.

A transverse magnetic-field component breaks axisymmetry leading to several new nonlinear effects. It “modulates” the flow structures found in the absence of a magnetic field (or in the presence of an axisymmetric field), such as Taylor vortex flow (TVF) and spiral vortex flow (SPI), generating so-called wavy Taylor vortices wTVF and wavy spiral vortices wSPI [6,22]. These new flow structures differ qualitatively from the classical flows found in the absence of magnetic fields [23,24].

The numerical results cited above all used the assumption that the internal magnetic field within the fluid was equal to the external applied field. In this paper, we show that, depending on the magnetic susceptibility of the ferrofluid in the annulus, there can be significant differences between the external and internal magnetic fields. We derive that the interaction between a uniform external field and the susceptibility of the ferrofluid-filled annulus results in a field with an  $r^{-2}$  radial dependence superimposed on the external field.

The paper is subdivided into four main parts. Following the introduction, Sec. II describes the model system and methods of investigation. That section also elucidates the differences between the internal and external fields and presents the rationale for the  $r^{-2}$  radial dependence. Further, we present the field equations for the magnetization and the velocity field and describe the implications of the magnetic terms in the generalized Navier-Stokes equations. Section III presents the main results, elucidating how the basic state and its primary instabilities, wTVF and wSPI, are influenced by a radial field dependence for transverse and oblique externally applied magnetic fields. We focus on stability and bifurcation properties and the spatiotemporal dynamics of the involved flow states. Further, we explain the stabilization effects of a radially dependent magnetic field. Finally, Sec. IV summarizes the main results and draws conclusions.

## II. SYSTEM AND THEORETICAL DESCRIPTION

The Taylor-Couette system (shown schematically in Fig. 1) consists of two concentric, independently rotating cylinders. The inner cylinder of radius  $r_1$  rotates at  $\omega_1$  and the outer cylinder of radius  $r_2$  rotates at  $\omega_2$ . Here, we consider periodic boundary conditions in the axial direction with periodicity of

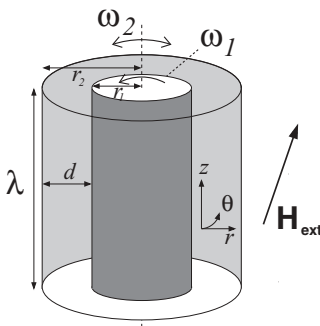


FIG. 1. Schematic of the Taylor-Couette system with an external applied homogeneous magnetic field  $\mathbf{H}_{\text{ext}}$ .

length  $\lambda$  and no-slip boundary conditions on the cylinders. The system is described using a cylindrical polar coordinate system  $(r, \theta, z)$  with a velocity field  $(u, v, w)$ . The radius ratio of the cylinders is set to  $\eta = r_1/r_2 = 0.5$  and the axial periodicity is set to  $\lambda/(r_2 - r_1) = 1.6$ . The gap between the cylinders is filled with a viscous, incompressible, isothermal ferrofluid. An external homogeneous magnetic field  $\mathbf{H}_{\text{ext}} = H_x \mathbf{e}_x + H_z \mathbf{e}_z$  is applied, where  $x = r \cos \theta$  is the transverse direction. Depending on the magnetic susceptibility of the ferrofluid in the annulus, this field is modified with an  $r^{-2}$  radial dependence (derived below). In the absence of a magnetic field, the basic flow is axisymmetric, but a magnetic field with a transverse component renders all states, including the basic state, to be nonaxisymmetric.

The flow dynamics of an incompressible homogeneous monodispersed ferrofluid with kinematic viscosity  $\nu$  and density  $\rho$  is governed by the incompressible Navier-Stokes equations, including magnetic terms, and the continuity equation. Using the gap  $d = (r_2 - r_1)$  as the length scale, the diffusion time  $\tau_D = d^2/\nu$  as the time scale, scaling pressure with  $\rho \nu^2/d^2$ , and the magnetic field  $\mathbf{H}$  and the magnetization  $\mathbf{M}$  with  $(\rho/\mu_0)^{0.5} \nu/d$  ( $\mu_0$  is the magnetic constant, i.e., magnetic permeability of free space), the nondimensional governing equations are

$$\begin{aligned} (\partial_t + \mathbf{u} \cdot \nabla) \mathbf{u} - \nabla^2 \mathbf{u} + \nabla p &= (\mathbf{M} \cdot \nabla) \mathbf{H} + \frac{1}{2} \nabla \times (\mathbf{M} \times \mathbf{H}), \\ \nabla \cdot \mathbf{u} &= 0. \end{aligned} \quad (2.1)$$

The cylinders are no-slip with velocity boundary conditions

$$\mathbf{u}(r_1, \theta, z) = (0, \text{Re}_1, 0) \text{ and } \mathbf{u}(r_2, \theta, z) = (0, \text{Re}_2, 0), \quad (2.2)$$

where the inner and outer Reynolds numbers are

$$\text{Re}_1 = \omega_1 r_1 d / \nu \text{ and } \text{Re}_2 = \omega_2 r_2 d / \nu. \quad (2.3)$$

Equation (2.1) is solved together with an equation that describes the magnetization of the ferrofluid. A first approximation is to use the equilibrium magnetization of an unperturbed state with a homogeneously magnetized ferrofluid at rest with the mean magnetic moments orientated in the direction of the magnetic field,  $\mathbf{M}^{\text{eq}} = \chi \mathbf{H}$ , where  $\chi$  is the magnetic susceptibility of the ferrofluid, determined using Langevin’s formula [25]. For the ferrofluid model used in this paper, corresponding to APG933 [26],  $\chi = 0.9$ . However, a ferrofluid’s magnetization is also influenced by the flow field. In our numerical simulations, we have used an approach based on the model of Niklas [4,5], as already presented in [6], where the magnetic fluid considered here is assumed to be incompressible, nonconducting, and to have a constant temperature and a homogeneous distribution of magnetic particles. We assume a stationary magnetization near equilibrium with small  $\|\mathbf{M} - \mathbf{M}^{\text{eq}}\|$  and small relaxation times  $\Omega \tau \ll 1$ , where  $\Omega$  is the absolute value of half of the vorticity  $\boldsymbol{\Omega}$  and  $\tau$  is the magnetic relaxation time. In the near-equilibrium approximation, Niklas [4] determined the relationship between the magnetization  $\mathbf{M}$ , the magnetic field  $\mathbf{H}$ , and the velocity  $\mathbf{u}$  to be

$$\mathbf{M} - \mathbf{M}^{\text{eq}} = c_N^2 \boldsymbol{\Omega} \times \mathbf{H}, \quad (2.4)$$

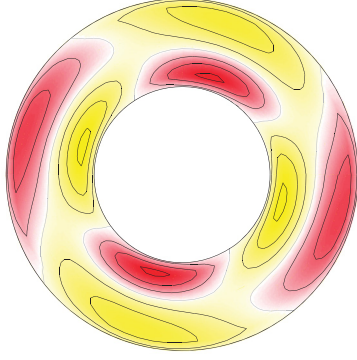


FIG. 2. (Color online) Contour plot of  $v - v_{\text{CCF}}$ , the difference between  $v_{\text{CCF}}$  and the azimuthal velocity component of the basic states for  $\text{Re}_1 = 60$  and  $\text{Re}_2 = 0$  with a transverse magnetic field  $T$  and  $\zeta = 0$ . Red (yellow) [dark (light gray)] contours correspond to positive (negative) values; the max (min) level is  $\pm 0.01$ .

where  $2\boldsymbol{\Omega} = \nabla \times \mathbf{u}$  is the vorticity, and the Niklas coefficient is

$$c_N^2 = \frac{\tau}{\left(\frac{1}{\chi} + \frac{\tau\mu_0 H^2}{6\mu\Phi}\right)}, \quad (2.5)$$

where  $\mu$  is the dynamic viscosity and  $\Phi$  is the volume fraction of the magnetic material.

#### A. Magnetic-field modification due to the ferrofluid-filled annulus

To solve the equation of motion Eq. (2.1) we have to consider the magnetic field within the annular gap between the cylinders. The simplest assumption is to take the magnetic field to be identical to the applied external field [4,6]. However, this simplest approach is only a leading-order approximation. Depending on the magnetic susceptibility of the ferrofluid, the magnetic field in the gap is modified.

Assuming infinitely long cylinders, the magnetic boundary conditions are

$$\mathbf{H} = \mathbf{H}_{\text{ext}} - M_r \mathbf{e}_r \quad \text{at } r = r_1 \quad \text{and } r = r_2, \quad (2.6)$$

where  $\mathbf{H}_{\text{ext}}$  is the homogeneous external applied magnetic field in the absence of the ferrofluid-filled annulus and  $M_r$  is the radial component of the magnetization  $\mathbf{M}$ .

A solenoidal field,  $\nabla \cdot \mathbf{H} = 0$ , can be satisfied by the following ansatz:

$$\mathbf{H} = \mathbf{H}_{\text{ext}} + [(a_1 - b_1/r^2) \cos \theta + (a_2 - b_2/r^2) \sin \theta] \mathbf{e}_r + [(a_2 + b_2/r^2) \cos \theta - (a_1 - b_1/r^2) \sin \theta] \mathbf{e}_\theta, \quad (2.7)$$

and then the boundary conditions defining the external field are

$$\mathbf{H}(r = r_1) = \mathbf{H}_{\text{ext}} + [(a_1 + b_1/r_1^2) \cos \theta + (a_2 + b_2/r_1^2) \sin \theta] \mathbf{e}_r + [(a_2 + b_2/r_1^2) \cos \theta - (a_1 + b_1/r_1^2) \sin \theta] \mathbf{e}_\theta, \quad (2.8)$$

and

$$\mathbf{H}(r = r_2) = \mathbf{H}_{\text{ext}} - (r_2/r)^2 [(a_1 + b_1/r_2^2) \cos \theta + (a_2 + b_2/r_2^2) \sin \theta] \mathbf{e}_r + (r_2/r)^2 [(a_2 + b_2/r_2^2) \cos \theta - (a_1 + b_1/r_2^2) \sin \theta] \mathbf{e}_\theta. \quad (2.9)$$

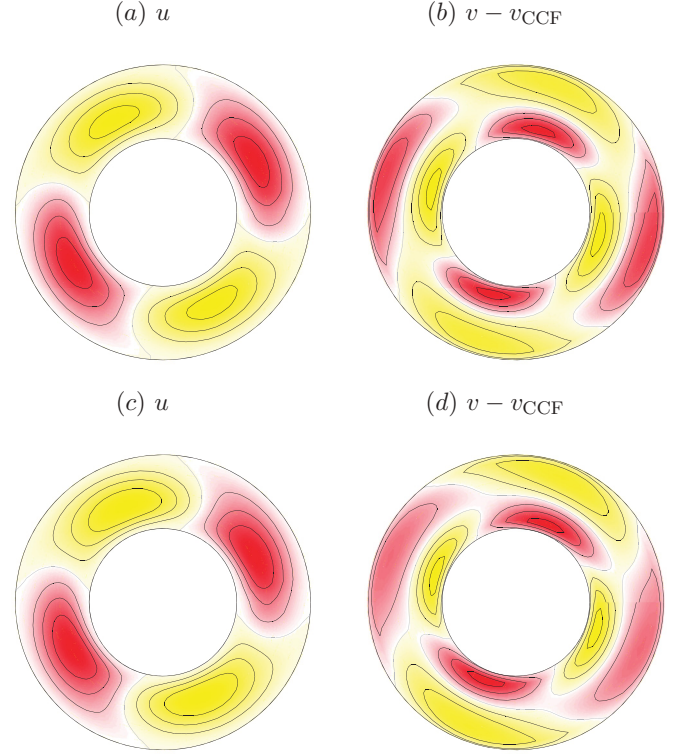


FIG. 3. (Color online) Contour plots of velocity components of the basic states,  $u$  and  $v - v_{\text{CCF}}$ , for  $\text{Re}_1 = 60$  and  $\text{Re}_2 = 0$  with a transverse magnetic field  $T$  for  $\zeta = 0.2$  (top row) and  $\zeta = 0.8$  (bottom row). Red (yellow) [dark (light gray)] contours correspond to positive (negative) values, with the max (min) for  $u$  being  $\pm 0.135\zeta$  and for  $v - v_{\text{CCF}}$  being  $\pm 0.33\zeta$ .

To calculate the four constants ( $a_1$ ,  $a_2$ ,  $b_1$ ,  $b_2$ ) from the boundary conditions Eq. (2.6), we need the radial component of the magnetization which results from substituting Eq. (2.7) into Eq. (2.4):

$$M_r = [\chi H_{\text{ext}}^T + \chi(a_1 - b_1/r^2) - c_N \Omega(a_2 + b_2/r^2)] \cos \theta + [c_N \Omega H_{\text{ext}}^T + \chi(a_2 - b_2/r^2) + c_N \Omega(a_1 + b_1/r^2)] \sin \theta, \quad (2.10)$$

where  $H_{\text{ext}}^T$  is the transverse component of  $\mathbf{H}_{\text{ext}}$ . Using the continuity of the magnetic-field condition on the cylinders,

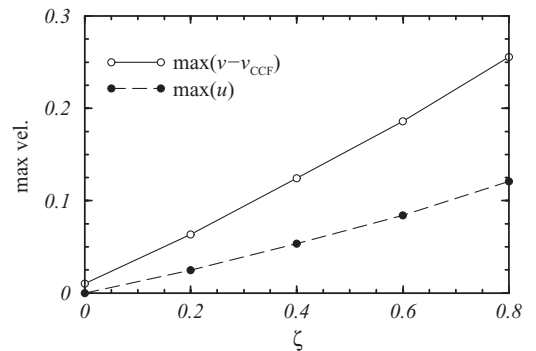


FIG. 4. Variation with  $\zeta$  of  $\max(u)$  and  $\max(v - v_{\text{CCF}})$  of the basic states at  $\text{Re}_1 = 60$  and  $\text{Re}_2 = 0$  in a transverse magnetic field  $T$ .

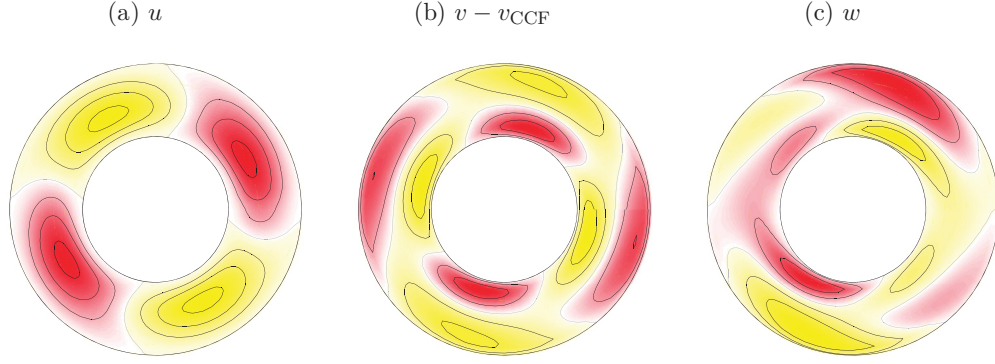


FIG. 5. (Color online) Contour plots of velocity components of the basic states  $u$ ,  $v - v_{\text{CCF}}$ , and  $w$  for  $\text{Re}_1 = 60$  and  $\text{Re}_2 = 0$  with an oblique magnetic field  $\mathcal{O}$  with  $\zeta = 0$ . Red (yellow) [dark (light gray)] contours correspond to positive (negative) values; the max (min) levels are for (a)  $\pm 0.02$ , (b)  $\pm 0.23$ , and (c)  $\pm 0.003$ .

the coefficients can be calculated. The resulting magnetic field is given by

$$\mathbf{H} = -\left(2H_{\text{ext}}^T/K\right)(r_1/r^2)\{[\chi \cos 2\theta + \Omega c_N \sin 2\theta]\mathbf{e}_x + [\chi \sin 2\theta - \Omega c_N \cos 2\theta]\mathbf{e}_y\}, \quad (2.11)$$

where  $K = (2 + \chi)^2 - \chi^2 \eta^2$ . A similar derivation of the modification of the magnetic field for a ferrofluid between two cylinders in the limit of equilibrium magnetization was presented in [20]. Their result is a special case of Eq. (2.11) when  $\Omega c_N = 0$ , corresponding to equilibrium magnetization.

### B. Ferrohydrodynamic equation of motion

The magnetization can be eliminated from Eq. (2.1) by using Eq. (2.4) to obtain the ferrohydrodynamic equation of motion [4]:

$$(\partial_t + \mathbf{u} \cdot \nabla)\mathbf{u} - \nabla^2 \mathbf{u} + \nabla p_M = -\frac{c_N^2}{2}(\mathbf{H}\nabla \cdot \mathbf{F} + \mathbf{H} \times \nabla \times \mathbf{F}), \quad (2.12)$$

where  $\mathbf{F} = \boldsymbol{\Omega} \times \mathbf{H}$  and  $p_M$  is the dynamic pressure incorporating all magnetic terms which can be written as gradients.

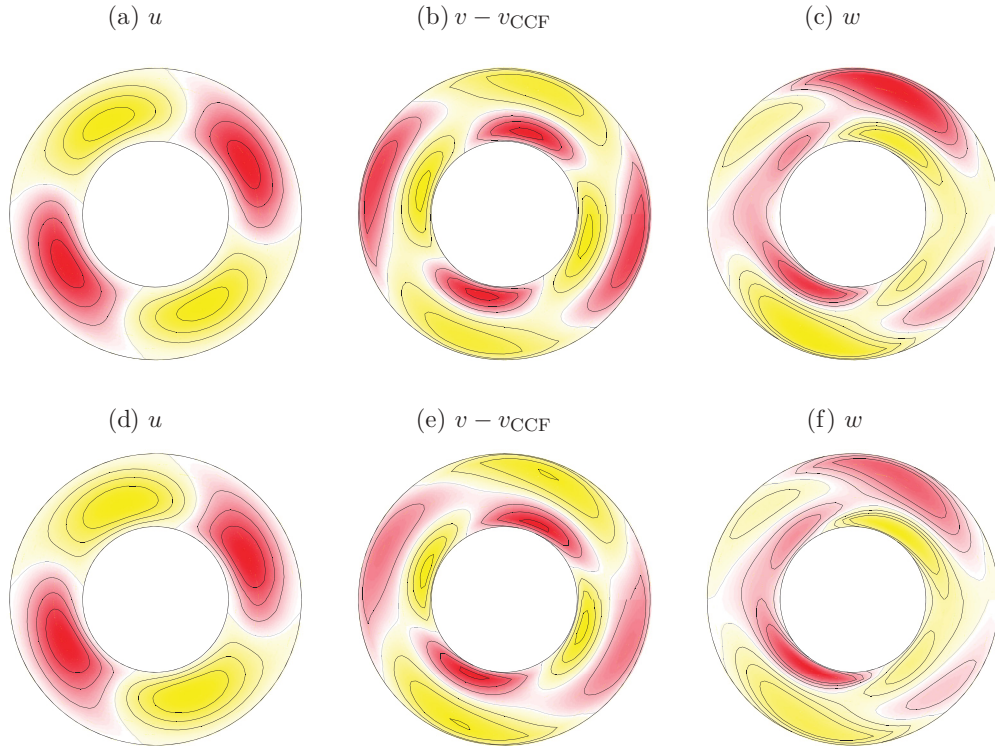


FIG. 6. (Color online) Contour plots of velocity components of the basic states  $u$ ,  $v - v_{\text{CCF}}$ , and  $w$ , in an  $(r, \theta)$  plane at  $z = 0$  for  $\text{Re}_1 = 60$  and  $\text{Re}_2 = 0$  with an oblique magnetic field  $\mathcal{O}$  for  $\zeta = 0.2$  (top row) and  $\zeta = 0.8$  (bottom row). Red (yellow) [dark (light gray)] contours correspond to positive (negative) values with the max (min) for  $u$  being  $\pm 0.15\zeta$ , for  $v - v_{\text{CCF}}$  being  $\pm 0.33\zeta$ , and for  $w$  being  $\pm 0.11\zeta$ .

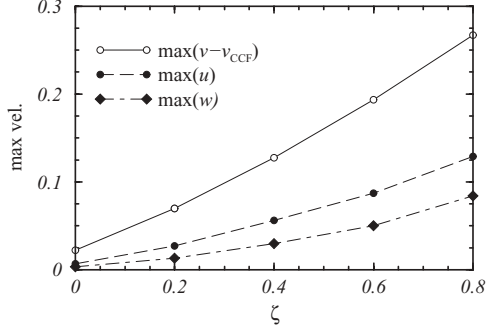


FIG. 7.  $\zeta$  dependence of  $\max(u)$ ,  $\max(v - v_{\text{CCF}})$ , and  $\max(w)$  for the basic states at  $\text{Re}_1 = 60$  and  $\text{Re}_2 = 0$  in an oblique magnetic field  $O$ .

From Eq. (2.11), we use the following magnetic field in the equation of motion:

$$\mathbf{H} = \frac{2(2 + \chi)}{K} H_x [(1 - \zeta/r^2) \cos \theta \mathbf{e}_r - \zeta/r^2 \sin \theta \mathbf{e}_\theta] + H_z \mathbf{e}_z, \quad (2.13)$$

where

$$\zeta = \frac{\chi}{2 + \chi} r_1^2 \quad (2.14)$$

characterizes the strength of the radial field dependence.

The magnetic-field strength and orientation are described by two parameters:

$$s_x = \frac{2(2 + \chi)}{K} H_x c_N \quad \text{and} \quad s_z = H_z c_N. \quad (2.15)$$

In this paper we only investigate magnetic fields with a transverse component  $s_x \neq 0$ . In particular, we present results for a pure transverse magnetic field,  $(s_x, s_z) = (0.6, 0.0)$ , denoted  $T$ , and an oblique magnetic field,  $(s_x, s_z) = (0.6, 0.6)$ , denoted  $O$ . These correspond to moderate magnetic fields used in several experiments [9,22].

### C. Numerical method

The ferrohydrodynamic system Eq. (2.12) is solved numerically with the code G1D3 [6]. G1D3 combines a finite difference method of second order in  $(r, z)$  and time (explicit)

with spectral decomposition in  $\theta$ :

$$f(r, \theta, z, t) = \sum_{m=-m_{\text{max}}}^{m_{\text{max}}} f_m(r, z, t) e^{im\theta}, \quad (2.16)$$

where  $f$  denotes one of  $\{u, v, w, p\}$ . For the parameter regimes studied here,  $m_{\text{max}} = 8$  provides adequate accuracy. We used homogeneous grids with discretization length  $\delta r = \delta z = 0.05$  and time steps  $\delta t < 1/3800$ . For diagnostic purposes, we also evaluate the complex mode amplitudes  $f_{m,n}(r, t)$  obtained from a Fourier decomposition in the axial direction:

$$f_m(r, z, t) = \sum_n f_{m,n}(r, t) e^{inkz}, \quad (2.17)$$

where  $k = 2\pi d/\lambda$  is the axial wave number.

## III. RESULTS

### A. Base state

In the presence of a pure axial magnetic field,  $H_{\text{ext}}(r)\mathbf{e}_z$ , the classical circular Couette flow (CCF), with  $\mathbf{u}_{\text{CCF}} = (0, Ar + B/r, 0)$ , where  $A = (\text{Re}_2 - \eta\text{Re}_1)/(1 + \eta)$  and  $B = \eta(\text{Re}_1 - \eta\text{Re}_2)/(1 + \eta)(1 - \eta)^2$ , is a solution of Eq. (2.12) as the associated vorticity  $\boldsymbol{\Omega}_{\text{CCF}} = \nabla \times \mathbf{u}_{\text{CCF}}$  is parallel to the magnetic field and therefore all magnetic terms vanish. For magnetic fields that are orientated purely in the radial or azimuthal direction, the basic state changes but remains axisymmetric with deviations from CCF only having an azimuthal component [4,27]. In all of these cases the basic state is invariant to a number of symmetries whose actions on a general velocity field are

$$R_\phi(u, v, w)(r, \theta, z) = (u, v, w)(r, \theta + \phi, z), \quad \phi \in [0, 2\pi), \quad (3.1)$$

$$K_z(u, v, w)(r, \theta, z) = (u, v, -w)(r, \theta, -z), \quad (3.2)$$

$$T_\alpha(u, v, w)(r, \theta, z) = (u, v, w)(r, \theta, z + \alpha), \quad \alpha \in \mathcal{R}. \quad (3.3)$$

For a field with a transverse component, the base state is no longer axisymmetric. We now present a brief description of these nonaxisymmetric basic states.

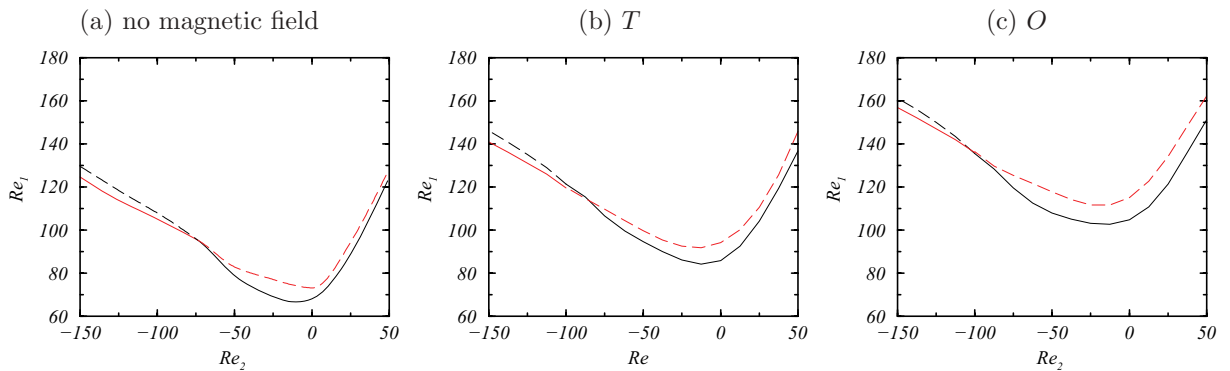


FIG. 8. (Color online) Bifurcation curves for the onset of (w)TVF (black) and (w)SPI [red (gray)] in  $\text{Re}_2$ - $\text{Re}_1$  parameter space for the Taylor-Couette problem with  $r_1/r_2 = 0.5$  and (a) no magnetic field, (b) an applied transverse field  $T$  with  $\zeta = 0$ , and (c) an applied oblique field  $O$  with  $\zeta = 0$  (the results are from [6,24]). Solid (dashed) lines indicate that the bifurcating solution is stable (unstable) at onset.

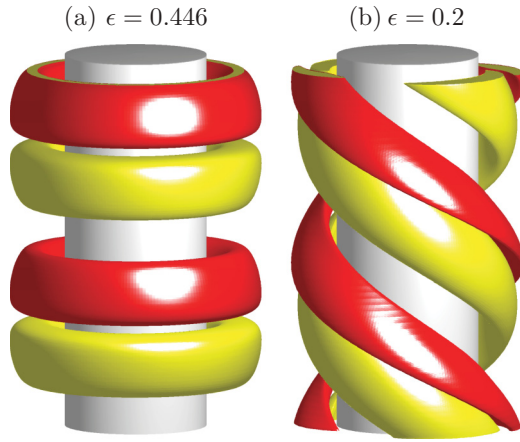


FIG. 9. (Color online) Azimuthal vorticity isosurfaces over two axial wavelengths with no applied magnetic field of (a) TVF at  $Re_2 = 0$  and  $Re_1 = 101.48$  and (b) SPI at  $Re_2 = -150$  and  $Re_1 = 151.98$ . Red (yellow) [dark (light gray)] isosurfaces correspond to positive (negative) values at (a)  $\pm 70$  and (b)  $\pm 90$ .

Figure 2 shows a contour plot of the difference between  $v_{CCF}$  and the azimuthal component  $v$  of the basic state velocity in a transverse magnetic field  $T$  for  $Re_1 = 60$ ,  $Re_2 = 0$ , and  $\zeta = 0$ . The radial and axial components remain zero and the basic state is invariant to  $K_z$  and  $T_\alpha$ , but the transverse magnetic field  $T$  breaks the axisymmetry  $R_\phi$ , resulting in a basic state with discrete symmetry  $R_\pi$ , i.e., with azimuthal wave number  $m = 2$ . Note that this  $m = 2$  state is stationary. This is in contrast to a generic breaking of an  $SO(2)$  symmetry which would result in a rotating wave.

Figure 3 shows contour plots of velocity components  $u$  and  $v - v_{CCF}$  of the basic state in a transverse magnetic field  $T$  for  $Re_1 = 60$  and  $Re_2 = 0$  and  $\zeta = 0.2$  (top row) and  $\zeta = 0.8$  (bottom row). So now, the magnetic field is not pure transverse since  $\zeta \neq 0$ , and a radial velocity component is generated by the radial magnetic-field dependence. However, the axial component remains zero and the basic state is still invariant to  $K_z$  and  $T_\alpha$ . The radial field dependence,  $\zeta$ , strengthens the

$m = 2$  azimuthal component. The  $v - v_{CCF}$  component is not much changed from the  $\zeta = 0$  case; the spatial structure is the same and its magnitude scales almost linearly with  $\zeta$ , as can be seen from the contour plots (Figs. 2 and 3). The radial velocity  $u$  also has an  $m = 2$  azimuthal symmetry. Its spatial structure is also approximately invariant with  $\zeta$  and its magnitude also scales almost linearly with  $\zeta$ . Figure 4 shows how the maxima of  $u$  and  $v - v_{CCF}$  vary with  $\zeta$ .

Figure 5 shows contour plots of velocity components  $u$ ,  $v - v_{CCF}$ , and  $w$  of the basic state in an oblique magnetic field  $O$  for  $Re_1 = 60$  and  $Re_2 = 0$ . Now, in addition to the  $m = 2$  wave due to the transverse component of the magnetic field, there is also an  $m = 1$  wave in the  $w$  field resulting from the coupling of the transverse and axial magnetic-field components (with a purely axial magnetic field, the  $u$  and  $w$  components remain zero [4,27]). In contrast to the case of an applied transverse magnetic field, here the basic state even for  $\zeta = 0$  has all components  $u$ ,  $v$ , and  $w$  being nonzero. The  $u$  and  $v$  components are still invariant to a rotation through  $\pi$  in  $\theta$ , but the  $w$  component is only  $2\pi$  periodic in  $\theta$  ( $m = 1$ ), although a rotation through  $\pi$  together with a change of sign leaves  $w$  invariant. This means that even though the axial component of the magnetic field is unidirectional the resulting axial flow is equal in both the positive and negative directions, so that while there is a zero mean (i.e., azimuthally averaged) axial flow there is strong shear in the axial direction [see Fig. 5(c)]. Again, the basic state is steady and invariant to  $K_z$  and  $T_\alpha$ , as in the case of the transverse field.

Figure 6 shows contour plots of  $u$ ,  $v - v_{CCF}$ , and  $w$  for the basic states at  $Re_1 = 60$  and  $Re_2 = 0$  in an oblique magnetic field  $O$  with  $\zeta = 0.2$  (top row) and  $\zeta = 0.8$  (bottom row). As for the case with a transverse field  $T$ , the radial field dependence  $\zeta$  strengthens the  $m = 2$  azimuthal component. The oblique field  $O$  also strengthens the  $m = 1$  azimuthal component, but only in the  $w$  component; the  $u$  and  $v$  components still have zero  $m = 1$  Fourier components (in fact, all of their odd Fourier components are zero). The symmetry of the basic state in the oblique field with  $\zeta \neq 0$  is unchanged from the  $\zeta = 0$  case. The spatial structure is also essentially invariant with  $\zeta$  and the magnitudes of the velocity components

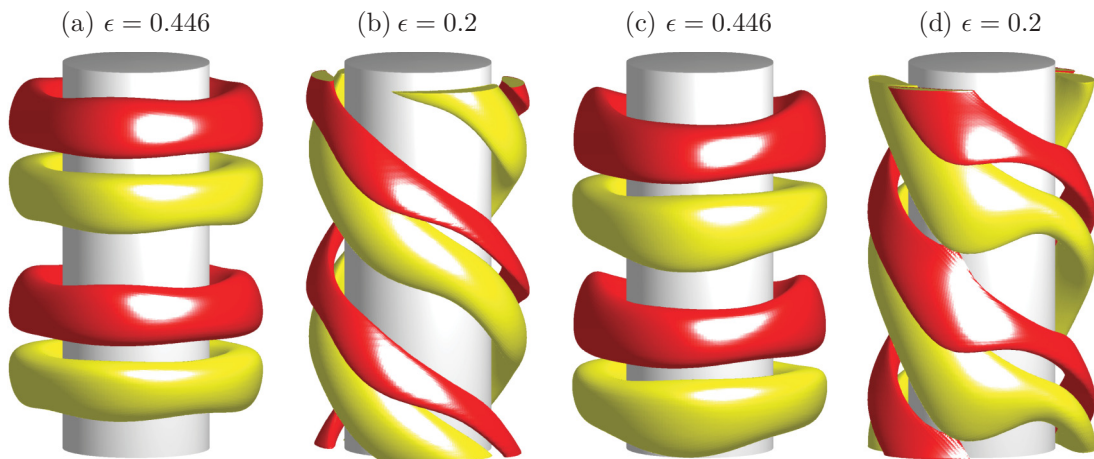


FIG. 10. (Color online) Azimuthal vorticity isosurfaces over two axial wavelengths for (a) wTVF at  $Re_2 = 0$  and  $Re_1 = 123$ , (b) wSPI at  $Re_2 = -150$  and  $Re_1 = 169$ , (c) wTVF at  $Re_2 = 0$  and  $Re_1 = 150$ , and (d) wSPI at  $Re_2 = -150$  and  $Re_1 = 188$ , all with  $\zeta = 0.0$ . Red (yellow) [dark (light gray)] isosurfaces correspond to positive (negative) values at (a)  $\pm 70$ , (b)  $\pm 90$ , (c),  $\pm 70$ , and (d)  $\pm 90$ .

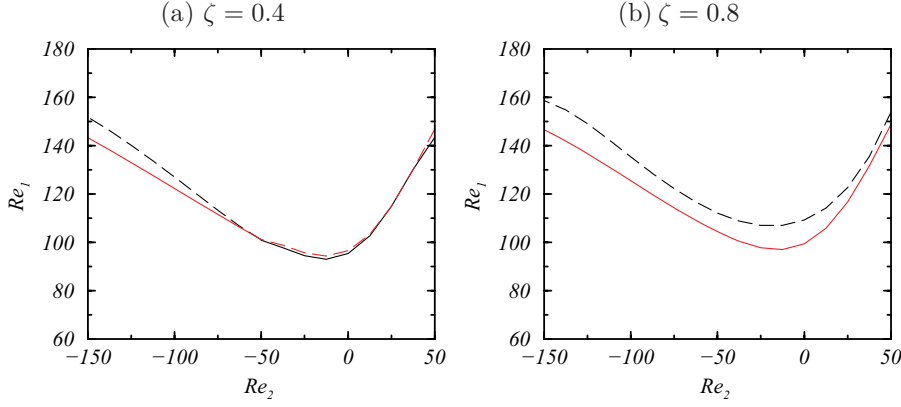


FIG. 11. (Color online) Bifurcation curves for the onset of wTVF (black) and wSPI [red (gray)] in  $(Re_2, Re_1)$  parameter space for different  $\zeta$  as indicated with an applied transverse magnetic field  $T$ .

vary almost linearly with  $\zeta$ , as can be seen both from the contour plots and Fig. 7, which shows how their maxima vary with  $\zeta$ .

### B. Primary instabilities of the basic state

Before embarking on a discussion of the effects of the radial field dependence  $\zeta$  on the instabilities of the basic state, we first summarize known results for  $r_1/r_2 = 0.5$  in the absence of a magnetic field [24], as well as the effects of a pure transverse and an oblique field with  $\zeta = 0$  [6], so as to give a baseline for assessing the effects of  $\zeta \neq 0$ .

Figure 8(a) shows the bifurcation curves in  $(Re_2, Re_1)$  space along which the basic state loses stability. When the counter rotation is sufficiently strong ( $Re_2 \lesssim -73$ ), the basic state, CCF, first becomes unstable to spiral vortex flow (SPI) in a supercritical Hopf bifurcation which breaks  $K_z$ , resulting in a pair of symmetrically related spiral states, one with left-handed winding and the other with right-handed winding. For  $Re_2$  presented here, the bifurcating SPI have an azimuthal wave number  $m = 1$  and their frequency close to onset varies from 25 to 35 depending on  $Re_2$ . For  $Re_2 \gtrsim -73$ , the basic state loses stability to the well-known Taylor vortex flow, TVF. The supercritical pitchfork of revolution bifurcation breaks  $T_\alpha$  and the steady axisymmetric family of solutions are parametrized by their axial location. A particular TVF and a left-winding SPI are shown as examples at points a little beyond critical in Fig. 9, showing isosurfaces of the azimuthal vorticity over two axial wavelengths. For ease of comparisons, we introduce the relative supercriticality of  $Re_1$  to the bifurcation threshold for

the vortex flow in question:

$$\epsilon = (Re_1 - Re_1^{\text{crit}})/Re_1^{\text{crit}}. \quad (3.4)$$

When a magnetic field with a transverse component is introduced, we have seen above that the basic state is changed from CCF. Figures 8(b) and 8(c) show the bifurcation curves for the instabilities of the altered basic states when a pure transverse field  $T$  or an oblique field  $O$ , both without radial dependency  $\zeta = 0$ , are applied. Just as the basic states were modified from CCF due to the applied magnetic fields, so are the primary instabilities, with TVF being replaced by a wavy Taylor vortex flow, wTVF, and SPI being replaced by wSPI. Their onset occurs at higher  $Re_1$  values for any given  $Re_2$  value compared to the onset of TVF and SPI in the absence of a magnetic field; i.e., the magnetic fields alter the basic states and makes them more robust to instabilities. The level of stabilization is greater when an oblique field is imposed compared to a purely transverse field. The codimension-two point at which the two bifurcation curves intersect is only slightly affected by the application of the magnetic fields, with a shift to stronger counter rotation, so that magnetic fields with  $\zeta = 0$  tend to render the corresponding basic states more unstable to wTVF. Figure 10 shows isosurfaces of the azimuthal vorticity of wTVF and wSPI in a transverse magnetic field  $T$  and an oblique magnetic field  $O$ , without any radial field dependence  $\zeta = 0$ . Details of these states have been reported in [6].

The question now is how does the radial field dependence  $\zeta$  affect the stability of the basic states and the characteristics of the bifurcating solutions. We begin by considering the purely

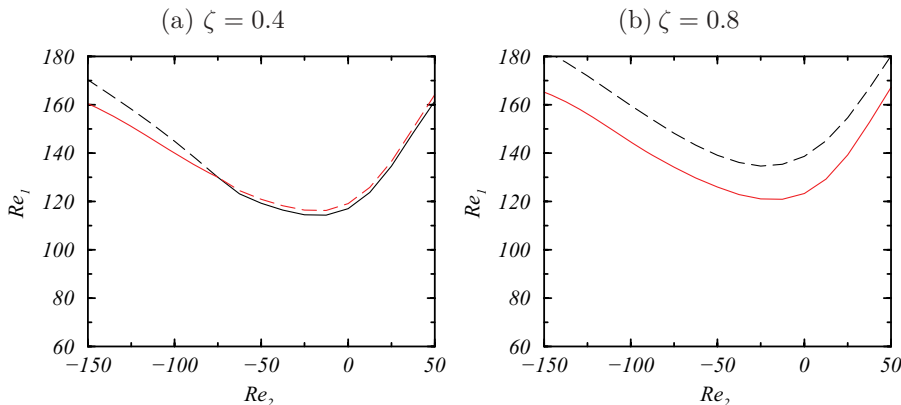


FIG. 12. (Color online) Bifurcation curves for the onset of wTVF (black) and wSPI [red (gray)] in  $(Re_2, Re_1)$  parameter space for different  $\zeta$  as indicated with an applied oblique magnetic field  $O$ .

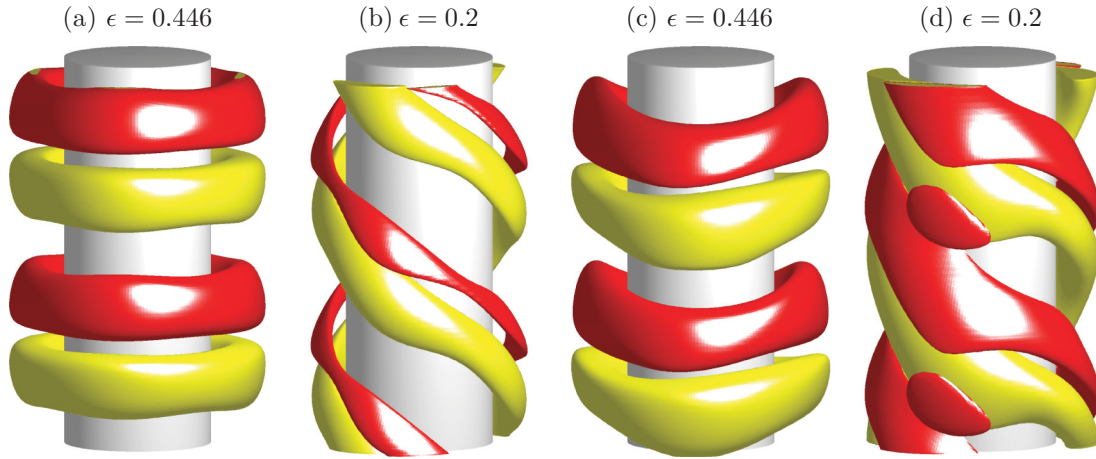


FIG. 13. (Color online) Azimuthal vorticity isosurfaces over two axial wavelengths for (a) wTVF at  $Re_2 = 0$  and  $Re_1 = 130$ , (b) wSPI at  $Re_2 = -150$  and  $Re_1 = 188$ , (c) wTVF at  $Re_2 = 0$  and  $Re_1 = 150$ , and (d) wSPI at  $Re_2 = -150$  and  $Re_1 = 196$ , all with  $\zeta = 0.8$ . Red (yellow) [dark (light gray)] isosurfaces correspond to positive (negative) values at (a)  $\pm 70$ , (b)  $\pm 90$ , (c)  $\pm 70$ , and (d)  $\pm 90$ .

transverse applied field  $T$ . Figure 11 shows the influence of the radial field parameter,  $\zeta$ , on the bifurcation thresholds for wTVF and wSPI in a transverse magnetic field  $T$ . The bifurcations continue being supercritical, as they were for  $\zeta = 0$ . The main effect that increasing  $\zeta$  has on the bifurcation curves is that the thresholds for the onset of both wTVF and wSPI are shifted to higher  $Re_1$ , with the threshold for wTVF being shifted significantly further. Aside from the enhanced stabilization of the basic state, there is an important consequence to the relative shifts in the two bifurcation curves. With the wTVF bifurcation curve being shifted more, the codimension-two point is also shifted to more positive  $Re_2$ , and by  $\zeta = 0.8$  we see that the codimension-two point is shifted to  $Re_2 > 50$ , so that the primary instability is the spiral wSPI, even with the two cylinders in strong corotation. This is a significant departure from classical Taylor-Couette flow both without magnetic fields and with uniform transverse or oblique fields applied. The radial field dependence, induced by the susceptibility of the ferrofluid-filled annulus, is seen to cause major changes in the quantitative and qualitative characteristics of the flow instabilities. This effect is even more pronounced when the applied field is oblique (see the corresponding bifurcation curves in Fig. 12). This is likely due to the axial component of the oblique field leading to a base state with  $w$  having axial shear, and the radial field dependence  $\zeta$  enhances the  $w$  component of the base state; this axial shear together with the base state azimuthal shear favors the spiral instability.

Figure 13 shows wTVF and wSPI in a transverse magnetic field  $T$  and an oblique magnetic field  $O$ , both with radial field dependence  $\zeta = 0.8$ . Compared to the  $\zeta = 0$  cases in Fig. 10, the modulations in all structures are enhanced. In general, the waviness of all flow structures is enhanced by the radial dependent magnetic field. Irrespective of the radial field dependence, the wTVF always remains a stationary nonrotating and phase pinned structure, whereas wSPI bifurcates either as a left- or right-winding spiral, depending on initial conditions. Their frequencies do not differ much

(about 20% or less) from those of SPI over the whole range of parameters we have considered here.

#### IV. CONCLUSION

When a magnetic field is applied across a container of ferrofluid, the ferrofluid's susceptibility modifies the structure of the magnetic field in the container. In modeling such problems, this modification is typically neglected. In this paper, we considered the dynamics of a ferrofluid in a Taylor-Couette apparatus subjected to a wide range of inner and outer cylinder rotations when a uniform external magnetic field is imposed. We derived how the field is modified, depending on the magnetic susceptibility, and then, over a range of susceptibilities from zero to values typical of commonly used ferrofluids, we determined how the basic state, its stability, and the primary bifurcating solutions are affected by the modifications to the imposed magnetic field. We focused on two field configurations, a purely transverse and an oblique field.

Due to the transverse nature of both field configurations, the basic state is not axisymmetric. For the purely transverse imposed field, ignoring the susceptibility-induced field modification gives a steady basic state with zero radial and axial velocity components, as in the classic circular Couette flow, but the azimuthal velocity is not axisymmetric. It has an azimuthal wave number  $m = 2$  dependence. The modified field introduces a nonzero radial velocity component, also with an  $m = 2$  azimuthal wave number, but the axial velocity component remains zero. The magnitudes of these  $m = 2$  velocity components scale almost linearly with the fluid's magnetic susceptibility.

With an imposed oblique magnetic field, the basic state has all velocity components being nonzero. The radial and azimuthal velocity components again have an  $m = 2$  azimuthal wave number, but the axial velocity has an  $m = 1$  azimuthal wave number. Even though the imposed magnetic field is unidirectional in the axial direction, the axial velocity is

not, leading to axial shear in the basic state. As with the purely transverse imposed field case, the nonaxisymmetric components of the basic state's velocity scale with the ferrofluid's susceptibility.

In the classic Taylor-Couette flow, the basic state is unstable to either centrifugal instability, leading to steady axisymmetric Taylor-Couette flow, TVF, or to a shear instability leading to time-periodic spiral vortex flow, SPI, depending on the relative rotation rates of the two cylinders. The spiral instability requires the cylinders to be in sufficiently strong counter rotation. With the imposed fields, we find a similar situation, with TVF and SPI being modified into wavy versions, wTVF and wSPI, due to the nonaxisymmetric nature of the basic state. Ignoring the susceptibility-induced modification to the magnetic field, the uniform imposed fields have a stabilizing effect on the basic state, with the switch between centrifugal

and shear instability being only slightly shifted compared to the zero-magnetic-field case. However, accounting for the susceptibility this switch is shifted to weaker counter rotations, especially with an oblique external field, and for susceptibilities typical of commonly used ferrofluids this shift is well into the corotating regime. This implies that in a typical experimental situation the primary instability will be observed as a shear-induced spiral flow. This is due to the increased axial shear in the axial velocity due to the oblique magnetic field.

#### ACKNOWLEDGMENTS

This work was supported by the World Class University program through the Korea Science and Engineering Foundation funded by the Ministry of Education, Science, and Technology (Grant No. R32-2009-000-20021-0).

- 
- [1] R. E. Rosensweig, *Ferrohydrodynamics* (Cambridge University Press, Cambridge, 1985).
- [2] J. E. Hart, *Dyn. Atmos. Oceans* **41**, 121 (2006).
- [3] J. E. Hart and S. Kittelman, *Dyn. Atmos. Oceans* **41**, 139 (2006).
- [4] M. Niklas, *Z. Phys. B* **68**, 493 (1987).
- [5] M. Niklas, H. Müller-Krumbhaar, and M. Lücke, *J. Magn. Magn. Mater.* **81**, 29 (1989).
- [6] S. Altmeyer, C. Hoffmann, A. Leschhorn, and M. Lücke, *Phys. Rev. E* **82**, 016321 (2010).
- [7] A. N. Vislovich, V. A. Novikov, and A. K. Sinitsyn, *J. Appl. Mech. Tech. Phys.* **27**, 72 (1986).
- [8] P. J. Stiles, M. Kagan, and J. B. Hubbard, *J. Colloid Interf. Sci.* **120**, 430 (1987).
- [9] O. Ambacher, S. Odenbach, and K. Stierstadt, *Z. Phys. B* **86**, 29 (1992).
- [10] J. E. Hart, *J. Fluid Mech.* **453**, 21 (2002).
- [11] J. Singh and R. Bajaj, *J. Magn. Magn. Mater.* **294**, 53 (2005).
- [12] A. Leschhorn, M. Lücke, C. Hoffmann, and S. Altmeyer, *Phys. Rev. E* **79**, 036308 (2009).
- [13] P. J. W. Debye, *Polar Molecules* (Dover, New York, 1929).
- [14] M. I. Shliomis, *Sov. Phys. JETP* **34**, 1291 (1972).
- [15] M. A. Martsenyuk, Y. L. Raikher, and M. I. Shliomis, *Sov. Phys. JETP* **38**, 413 (1974).
- [16] M. I. Shliomis, *Phys. Rev. E* **64**, 060501 (2001).
- [17] M. I. Shliomis, *Phys. Rev. E* **64**, 063501 (2001).
- [18] H. W. Müller and M. Liu, *Phys. Rev. E* **64**, 061405 (2001).
- [19] B. U. Felderhof, *Phys. Rev. E* **62**, 3848 (2000).
- [20] S. Odenbach and H. W. Müller, *Phys. Rev. Lett.* **89**, 037202 (2002).
- [21] M. Reindl, A. Leschhorn, M. Lücke, and S. Odenbach, *J. Phys.: Conf. Ser.* **149**, 012109 (2009).
- [22] M. Reindl and S. Odenbach, *Phys. Fluids* **23**, 093102 (2011).
- [23] M. Golubitsky and W. F. Langford, *Physica D* **32**, 362 (1988).
- [24] C. Hoffmann, S. Altmeyer, A. Pinter, and M. Lücke, *New J. Phys.* **11**, 053002 (2009).
- [25] P. Langevin, *Ann. Chim. Phys.* **5**, 70 (1905).
- [26] J. Embs, H. W. Müller, C. Wagner, K. Knorr, and M. Lücke, *Phys. Rev. E* **61**, R2196 (2000).
- [27] S. Odenbach and G. H., *J. Magn. Magn. Mater.* **152**, 123 (1995).